VICTORIA UNIVERSITY OF TECHNOLOGY

DEPARTMENT OF COMPUTER AND MATHEMATICAL SCIENCES

Three Configurations of Block Edge Detections for Binary Images of Hexagonal Grid

Z. J. Zheng

(39 COMP 11)

April 1994

TECHNICAL REPORT

VICTORIA UNIVERSITY OF TECHNOLOGY
(P O BOX 14428) MELBOURNE MAIL CENTRE
MELBOURNE, VICTORIA, 3000
AUSTRALIA

TELEPHONE (03) 688 4249 / 4492
FACSIMILE (03) 688 4050

Footscray Campus

Three Configurations of Block Edge Detections for Binary Images of the Hexagonal Grid

Z.J. Zheng

Department of Computer and Mathematical Sciences, Victoria University of Technology

Footscray, Vic. 3000, Australia

Abstract

Three configurations of block edge detections based on the third level of the conjugate classification for binary images of the hexagonal grid, are investigated in this paper. Constructing an operation of three configurations, it is necessary to collect a state set contained 48, 66 and 90 states as the structuring patterns respectively. To represent the selected state set in equivalent detecting functions, cellular logic and conjugate functions are illustrated and compared. Because a conjugate function uses a class representation for structuring patterns, its real implementation is very efficient. For three configurations of 0 (or 1) block edge detections, a speed-up ratio 6-15 compared with the same activity performed by a standard implementation in a cellular logic function, can be measured. Sample processed pictures and their timing measurements are illustrated and analyzed.

Key Words: cellular logic computation, structuring patterns, pattern recognition, block edge detection, computational complexity, conjugate classification and transformation.

1 Introduction

For any binary image, various edge and line structure components play the most eminent role in analyzing binary images [Kong and Rosenfeld 1989, Serra 1982]. Many practical analysis tasks strongly depend on different edge detections such as in computer vision and pattern recognition applications. An efficient scheme of simple block edge detection for the hexagonal grid has been investigated by the author [Zheng 1993a]. The conjugate transformation for binary images of the hexagonal grid was proposed by Zheng and Maeder (1993). An efficient scheme for simple line component detections (or simple network detection) on the hexagonal grid is examined by Zheng (1993b) and three configurations of network detections for binary images of the hexagonal grid are investigated by Zheng (1993c). In this paper, three configurations of block edge detections are presented. Their detecting functions and time complexity measures of the implementations are compared.

How to separate 0 or 1 block edge components - *block edges* - from other parts is a difficult and practical problem in many image analysis and pattern recognition applications. Since multiple structuring patterns of a 2D binary image have to be selected from a given grid, it is possible to use different invariants such as rotational invariant to organize all involved states into classes [Golay 1969, Zheng and Maeder 1992]. The possible number of structuring patterns for general block edge points is larger than the possible number of structuring patterns for specific block edge points. It is necessary to investigate the family of block edge detections from simple to complex in a hierarchy to deeply understand the properties involved in these operations.

For most practical applications, operations of block edge detections are relevant to operations detecting all clear block edge-oriented patterns (or *simple block edges*). However, huge practical applications of computer vision and pattern recognition depend on either intermediate or final results of thinning or skeleton operations. During thinning or skeleton procedures, if we want to perform a block edge detection, then in addition to simple block edge points, it is essential to concern other mixed points such as line and block edge intersection points to identify *extensive* block edge points contained more intersection patterns than simple block edge detection. Using cellular logic expression, there is a standard implementation to detect a selected state set. In a canonical form of these expressions, if there are n states selected and each state requires t binary operations, then a total of $n \times t$ binary operations are expected to determine a block edge point dependent on the selected state set.

Three configurations of block edge detections for binary images of the hexagonal grid is investigated in this paper which is divided into following sections. In section two, three clumps (primitive classes of states) of block edge detections on the hexagonal grid are defined and examined. The state sets needed to be selected for a family of block edge detections are investigated. In addition, the symmetric operations used to manage the relevant state set are investigated. In section three, cellular logic and conjugate equations are used to express each detection function in a canonical expression. Their theoretical complexities and speed-up ratios are analyzed. In section four, sample pictures of three configurations of block edge detections and their real time measurements are illustrated. Theoretical and real speed-up ratios are illustrated; and finally in section five the main contributions of the paper are summarized.

2 Primitive Classes of Block Edge Detections

To gain a clear explanation of block edge detection, it is convenient to start from a relevant example. First, the problem of block edge detection is examined using sample pictures in Figure 1 (a)-(c). Figure 1(a) is a sample image composed of other structures (isolated, inner and network components) and 1-block edges. It has been separated into other structures in Figure 1(b) and 1-block edges in Figure 1(c). If we restrict the image to the hexagonal grid, is it feasible to perform similar operations mechanically?

2.1 The Kernel Form of the Hexagonal Grid

To answer this question, it is necessary to analyze how many structuring patterns are required for block edge detection.

Let X denoted a binary image on the hexagonal grid, $x \in X$ be a given point of the image. The simplest scheme for block edge detection on the hexagonal grid uses seven adjacent grid points (the kernel form of the hexagonal grid) as the structuring form. The kernel form is a regular form composed of seven grid points for which one point x is at the centre and another six neighbouring points $x_0 - x_5$ are around it. The kernel form can be denoted by $K(x)$ shown in Figure 2. Each point is allowed to assume values of only 1 or 0; seven points have fixed values as a state (structuring pattern), and there is a total of 128 states as a state set denoted as $\mathcal{G}(K(x))$ for the kernel form.

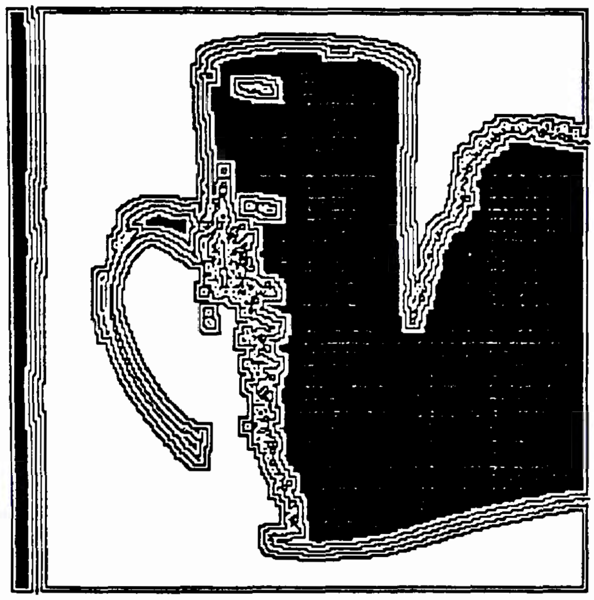

(a) Original Image

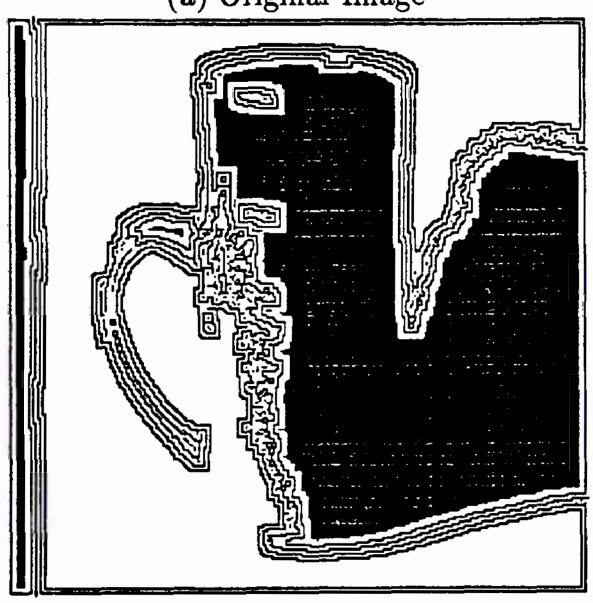

(b) Other Components

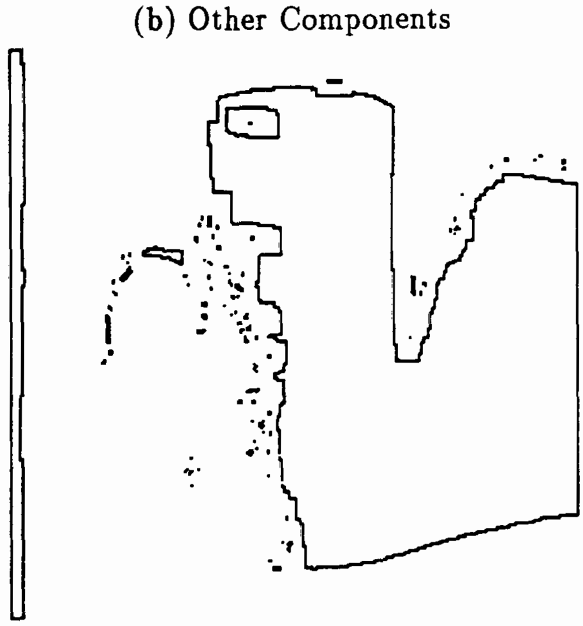

(c) 1-Block Edges

Figure 1: Identifying 1-Block Edge Components from a Binary Image (a)-(c).

$$K(x) = \begin{matrix} & x_0 & & x_1 & \\ x_5 & & x & & x_2 \\ & x_4 & & x_3 & \end{matrix} = (x, \cdots, x_i, \cdots, x_1, x_0) = (x_6, \cdots, x_i, \cdots, x_1, x_0),$$

$$x_i \in \{0,1\}, \quad 0 \le i \le 6, \quad x \in X.$$

Figure 2: The Kernel Form of the Hexagonal Grid

2.2 Different Block Edge Points

For any point x of a binary image on the hexagonal grid, it is a *block edge* point if it has at least two neighbouring points in a run which have the same value as x and there is at least one neighbouring point in opposite value. It is a *simple block edge* point, if it is a block edge point and all neighbouring points which have the same value as x are arranged as one run and other neighbouring points with the opposite value in another run. It is an *extensive block edge* point, if it is a block edge point and there are more than two runs of neighburing points in the same value as x.

2.3 Three Clumps of Block Edge Patterns

In order to satisfy the requirements of detecting 1-block edges, the following state sets have to be selected as the structuring patterns. There are eight rotational invariant classes with a total of 45 states in three clumps - first clump: 24 states in four classes for simple block edge patterns; second clump: nine states in two classes for extensive block edge patterns with two runs (3-1 and 2-2 runs) and third clump: 12 states in one class for extensive block edge patterns for two runs (2-1 and 1-2 runs) respectively shown in Figure 3. Conversely, for describing 0-block edges, another three clumps of the conjugate state sets have to be selected as the structuring patterns. There are eight rotational invariant classes with a total of 45 states too shown in Figure 4.

Because a block edge is composed of three clumps of states in 16 rotational invariant classes, it is necessary for representations of both 0 and 1 block edges to select a total of 90 states as structuring

Structuring Patterns of 1-Block Edges:
First Clump - 24 Patterns in Four Classes

$$\left\{ \begin{array}{ccccc} & 1 & & 1 & \\ 0 & & 1 & & 0 \\ & 0 & & 0 & \end{array}, \begin{array}{ccccc} & 0 & & 1 & \\ 0 & & 1 & & 1 \\ & 0 & & 0 & \end{array}, \dots, \begin{array}{ccccc} & 1 & & 0 & \\ 1 & & 1 & & 0 \\ & 0 & & 0 & \end{array} \right\};$$

$$\left\{ \begin{array}{ccccc} & 1 & & 1 & \\ 0 & & 1 & & 1 \\ & 0 & & 0 & \end{array}, \begin{array}{ccccc} & 0 & & 1 & \\ 0 & & 1 & & 1 \\ & 0 & & 1 & \end{array}, \dots, \begin{array}{ccccc} & 1 & & 1 & \\ 1 & & 1 & & 0 \\ & 0 & & 0 & \end{array} \right\};$$

$$\left\{ \begin{array}{ccccc} & 1 & & 1 & \\ 0 & & 1 & & 1 \\ & 0 & & 1 & \end{array}, \begin{array}{ccccc} & 0 & & 1 & \\ 0 & & 1 & & 1 \\ & 1 & & 1 & \end{array}, \begin{array}{ccccc} & 1 & & 1 & \\ 1 & & 1 & & 1 \\ & 0 & & 0 & \end{array} \right\};$$

$$\left\{ \begin{array}{ccccc} & 1 & & 1 & \\ 0 & & 1 & & 1 \\ & 1 & & 1 & \end{array}, \begin{array}{ccccc} & 0 & & 1 & \\ 1 & & 1 & & 1 \\ & 1 & & 1 & \end{array}, \dots, \begin{array}{ccccc} & 1 & & 1 & \\ 1 & & 1 & & 1 \\ & 0 & & 1 & \end{array} \right\}.$$

Second Clump - Nine Patterns in Two Classes

$$\left\{ \begin{array}{ccccc} & 1 & & 1 & \\ 0 & & 1 & & 1 \\ & 1 & & 0 & \end{array}, \begin{array}{ccccc} & 0 & & 1 & \\ 1 & & 1 & & 1 \\ & 0 & & 1 & \end{array}, \dots, \begin{array}{ccccc} & 1 & & 1 & \\ 1 & & 1 & & 0 \\ & 0 & & 1 & \end{array} \right\};$$

$$\left\{ \begin{array}{ccccc} & 1 & & 1 & \\ 0 & & 1 & & 0 \\ & 1 & & 1 & \end{array}, \begin{array}{ccccc} & 0 & & 1 & \\ 1 & & 1 & & 1 \\ & 1 & & 0 & \end{array}, \begin{array}{ccccc} & 1 & & 0 & \\ 1 & & 1 & & 1 \\ & 0 & & 1 & \end{array} \right\};$$

Third Clump - 12 Patterns in Two Classes

$$\left\{ \begin{array}{ccccc} & 1 & & 1 & \\ 0 & & 1 & & 0 \\ & 1 & & 0 & \end{array}, \begin{array}{ccccc} & 0 & & 1 & \\ 1 & & 1 & & 1 \\ & 0 & & 0 & \end{array}, \dots, \begin{array}{ccccc} & 1 & & 0 & \\ 1 & & 1 & & 0 \\ & 0 & & 1 & \end{array} \right\};$$

$$\left\{ \begin{array}{ccccc} & 1 & & 1 & \\ 0 & & 1 & & 0 \\ & 0 & & 1 & \end{array}, \begin{array}{ccccc} & 0 & & 1 & \\ 0 & & 1 & & 1 \\ & 1 & & 0 & \end{array}, \dots, \begin{array}{ccccc} & 1 & & 0 & \\ 1 & & 1 & & 1 \\ & 0 & & 0 & \end{array} \right\};$$

Figure 3: Three Clumps of Structuring Patterns for 1-Block Edges

Structuring Patterns of 0-Block Edges:
First Clump - 24 Patterns in Four Classes

$$\left\{ \begin{array}{ccccc} & 0 & & 0 & \\ 1 & & 0 & & 1 \\ & 1 & & 1 & \end{array}, \begin{array}{ccccc} & 1 & & 0 & \\ 1 & & 0 & & 0 \\ & 1 & & 1 & \end{array}, \cdots, \begin{array}{ccccc} & 0 & & 1 & \\ 0 & & 0 & & 1 \\ & 1 & & 1 & \end{array} \right\};$$

$$\left\{ \begin{array}{ccccc} & 0 & & 0 & \\ 1 & & 0 & & 0 \\ & 1 & & 1 & \end{array}, \begin{array}{ccccc} & 1 & & 0 & \\ 1 & & 0 & & 0 \\ & 1 & & 0 & \end{array}, \cdots, \begin{array}{ccccc} & 0 & & 0 & \\ 0 & & 0 & & 1 \\ & 1 & & 1 & \end{array} \right\};$$

$$\left\{ \begin{array}{ccccc} & 0 & & 0 & \\ 1 & & 0 & & 0 \\ & 1 & & 0 & \end{array}, \begin{array}{ccccc} & 1 & & 0 & \\ 1 & & 0 & & 0 \\ & 0 & & 0 & \end{array}, \cdots, \begin{array}{ccccc} & 0 & & 0 & \\ 0 & & 0 & & 0 \\ & 1 & & 1 & \end{array} \right\};$$

$$\left\{ \begin{array}{ccccc} & 0 & & 0 & \\ 1 & & 0 & & 0 \\ & 0 & & 0 & \end{array}, \begin{array}{ccccc} & 1 & & 0 & \\ 0 & & 0 & & 0 \\ & 0 & & 0 & \end{array}, \cdots, \begin{array}{ccccc} & 0 & & 0 & \\ 0 & & 0 & & 0 \\ & 1 & & 0 & \end{array} \right\}.$$

Second Clump - Nine Patterns in Two Classes

$$\left\{ \begin{array}{ccccc} & 0 & & 0 & \\ 1 & & 0 & & 0 \\ & 0 & & 1 & \end{array}, \begin{array}{ccccc} & 1 & & 0 & \\ 0 & & 0 & & 0 \\ & 1 & & 0 & \end{array}, \cdots, \begin{array}{ccccc} & 0 & & 0 & \\ 0 & & 0 & & 1 \\ & 1 & & 0 & \end{array} \right\};$$

$$\left\{ \begin{array}{ccccc} & 0 & & 0 & \\ 1 & & 0 & & 1 \\ & 0 & & 0 & \end{array}, \begin{array}{ccccc} & 1 & & 0 & \\ 0 & & 0 & & 0 \\ & 0 & & 1 & \end{array}, \begin{array}{ccccc} & 0 & & 1 & \\ 0 & & 0 & & 0 \\ & 1 & & 0 & \end{array} \right\};$$

Third Clump - 12 Patterns in Two Classes

$$\left\{ \begin{array}{ccccc} & 0 & & 0 & \\ 1 & & 0 & & 1 \\ & 1 & & 0 & \end{array}, \begin{array}{ccccc} & 1 & & 0 & \\ 1 & & 0 & & 0 \\ & 0 & & 1 & \end{array}, \cdots, \begin{array}{ccccc} & 0 & & 1 & \\ 0 & & 0 & & 0 \\ & 1 & & 1 & \end{array} \right\};$$

$$\left\{ \begin{array}{ccccc} & 0 & & 0 & \\ 1 & & 0 & & 1 \\ & 0 & & 1 & \end{array}, \begin{array}{ccccc} & 1 & & 0 & \\ 0 & & 0 & & 0 \\ & 1 & & 1 & \end{array}, \cdots, \begin{array}{ccccc} & 0 & & 1 & \\ 0 & & 0 & & 1 \\ & 1 & & 0 & \end{array} \right\};$$

Figure 4: Three Clumps of Structuring Patterns for 0-Block Edges

patterns. If we could get a simpler organization to identify these block edge states, then it is helpful for block edge detection to get an efficient algorithm. Therefore, the requirements of looking for efficient operations of block edge detections force us to investigate proper representations of the state set of the kernel form of the hexagonal grid. From the above discussion, we can establish the following lemma.

Lemma 2.3.1 *For any binary image of the hexagonal grid, if the kernel form of the grid is selected as the structuring form and three clumps of block edge patterns need to be identified, then it is necessary to select 90 structuring patterns from its 128 state set. The selected structuring patterns belong to 16 rotational invariant classes and each class contains three to six states.*

Proof: No other states can be identified as block edge state from the hexagonal grid in relation to the kernel form except selected states in Figures 3-4. Three clumps of state sets shown in Figures 3-4 contain all state set relevant to 0 and 1 block edge points. Each number of a class can be counted directly. □

From an algebraic viewpoint, three operations can be identified to transform the structuring patterns of block edge detections. The first one is the conjugation which establishes 0 to 1 and 1 to 0 symmetry. The second one is the number of connections and the third one is the number of branches. Three conditions play the key role for the problem of block edge detections.

2.4 The Conjugate Classification of the Kernel Form

The conjugate classification of the kernel form of the hexagonal grid is established by Zheng and Maeder (1992) and further systematic investigations are shown in [Zheng Thesis 1994]. For a convenience in description, the classification can be briefly described as follows:

The *kernel form* $K(x)$ of the hexagonal grid is a point x with six neighbouring points around it. When each point is allowed to assume values of only 0 or 1, there is a total of 128 states corresponding to unique instances of the kernel form. From the state set $\mathcal{G}(K(x))$ of 128 states and the inclusion relation of set theory, we can use a hierarchy of six levels to represent the conjugate classification. Each level contains 128 states and each node is a subset of states. Any two nodes in the same level do not contain the same state. If we let $\mathcal{G}(K(x))$ be the root, then the first level can be divided into one state set G and one conjugate state set $\widetilde{G}$ dependent on the value of the centre point x, $x \in \{0,1\}$. The second level of 14 nodes $\{_pG,_p\widetilde{G}\}$ can be distinguished by p, the number of connections, $0 \leq p \leq 6$, that is, the number of six neighbouring points with the same value of the centre point. The third level of 22 nodes $\{^q_pG\}$ and $\{^q_p\widetilde{G}\}$ is related to q which corresponds to the number of branches, $0 \leq q \leq 3$ (the number of runs of the six neighbouring points with the same value of the centre point in each state). The fourth level of 28 nodes $\{^q_pG^s\}$ and $\{^q_p\widetilde{G}^s\}$ has the property of rotational invariant in which any two states in a node can be congruent by rotation, and s denotes the number of spins, $s \in \{-1,0,1\}$. Only six nodes for $q=2$ need to be identified using s. The fifth level of 128 leaves $\{^q_pG^s_r\}$ and $\{^q_p\widetilde{G}^s_r\}$ has a simple relation to the respected state, and r denotes the number of rotations $0 \leq r \leq 6$. In short, the conjugate classification is a hierarchy of six levels: one root, two nodes, 14 nodes, 22 nodes, 28 nodes and 128 leaves. Each node of the hierarchy is a class of states with 1-5 calculable parameters. The whole structure of the classification has been represented by (x,p,q,s,r) which denote five calculable parameters of this classification [Zheng and Maeder 1992]. For convenience, each intermediate node is called a class too.

2.5 The Proper Level for Block Edge Detections

The hierarchical structure of the conjugate classification provides a flexible framework for supporting different applications. It is obvious that x or (x,p) is not enough to describe the selecting block edge classes. However, it is possible to use three parameters (x,p,q) for the description.

We need some explanations to determine which level is a proper level of the conjugate classification for an arbitrary operation of block edge detections. If states in first to third clumps need to be selected, it is necessary and sufficient to use the third level: (x,p,q). Owing to this reason, we use the third level of the conjugate classification to implement required operations, that is, the substructure of the conjugate classification involving 22 nodes $\{^q_pG\}$ and $\{^q_p\widetilde{G}\}$.

The third level of the conjugate classification is illustrated in Figure 5. Some details of two nodes are explained in Figure 5(a), and their 22 nodes are shown in Figure 5(b).

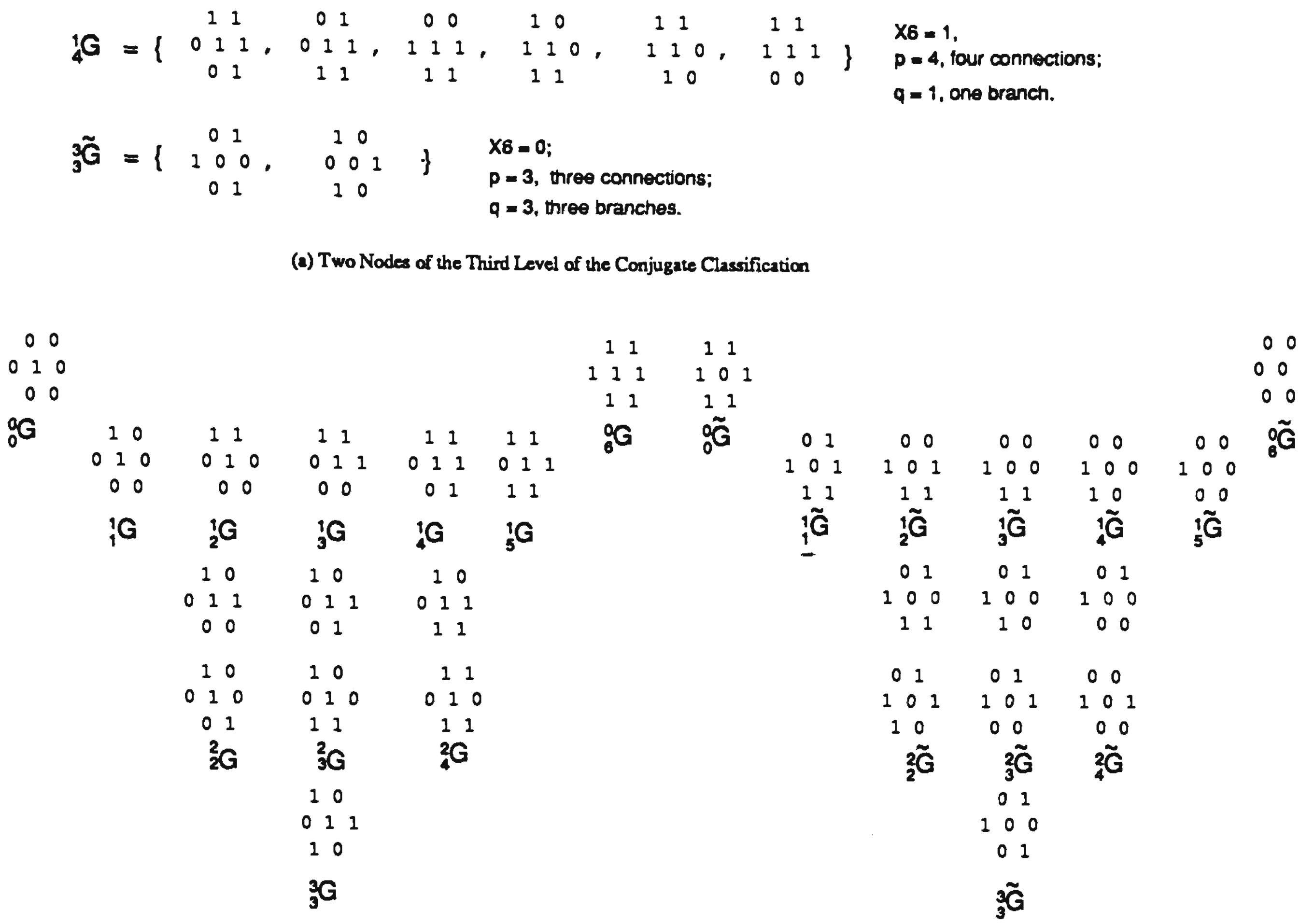

(a) Two Nodes of the Third Level of the Conjugate Classification

(b) The 22 Nodes of the Third Level of the Conjugate Classification

Figure 5: The Third Level of the Conjugate Classification

In order to describe the selected structuring patterns, only $\{^1_2G, ^1_3G, ^1_4G, ^1_5G, ^2_4G, ^2_3G, ^1_2\tilde{G}, ^1_3\tilde{G}, ^1_4\tilde{G}, ^1_5\tilde{G}, ^2_4\tilde{G}, ^2_3\tilde{G}\}$ nodes of the third level of the conjugate classification, are relevant. Their combinations can satisfy the most applications of block edge detection relevant to the first to third clumps.

Proposition 2.5.1 *The third level of the conjugate classification can provide a necessary representation for the 16 classes of block edge points of the hexagonal grid.*

Proof: The third level of structure contains 12 nodes relevant to selected 16 classes that can be distinguished from each other. It is necessary to support most combinations of these classes. Neither $(x,p),(x,q),(p,q)$ nor $(x),(p),(q)$ can represent the required classes. So it is necessary for a block edge detection to use the third level. □

2.6 Three Configurations of Block Edge Detections

Since we can select a subset of 12 nodes from the third level to generate an operation of block edge detections. It is necessary to declare what are three configurations in our investigation.

Let $\mathcal{A}_i$ or $\mathcal{B}_i \subset \mathcal{G}(K(x))$ denote the block edge state set of the i-th configuration, $0 \leq i \leq 2$. Six block edge state sets can be defined as follows:

$$\mathcal{A}_0 = \{{}^1_2G, {}^1_3G, {}^1_4G, {}^1_5G\}; \tag{1}$$

$$\mathcal{B}_0 = \{{}^1_2\widetilde{G}, {}^1_3\widetilde{G}, {}^1_4\widetilde{G}, {}^1_5\widetilde{G}\}; \tag{2}$$

$$\mathcal{A}_1 = \{\mathcal{A}_0, {}^2_4G\}; \tag{3}$$

$$\mathcal{B}_1 = \{\mathcal{B}_0, {}^2_4\widetilde{G}\}; \tag{4}$$

$$\mathcal{A}_2 = \{\mathcal{A}_1, {}^2_3G\}; \tag{5}$$

$$\mathcal{B}_2 = \{\mathcal{B}_1, {}^2_3\widetilde{G}\}. \tag{6}$$

As for the previous investigations for block edge points of three clumps, three configurations correspond the best possibility to use three clumps on the third level of the conjugate classification for block edge detection.

Let $|\mathcal{A}_i|$ denote the number of states in $\mathcal{A}_i$, we have

$$|\mathcal{A}_0| = |\mathcal{B}_0| = 24; \tag{7}$$

$$|\mathcal{A}_1| = |\mathcal{B}_1| = 33; \tag{8}$$

$$|\mathcal{A}_2| = |\mathcal{B}_2| = 45. \tag{9}$$

For convenience in representations on the third level, we use above three configurations to construct six operations for block edge detections.

3 Expressions for Block Edge Detections

In this section, detecting expressions in relation to both cellular logic and conjugate functions are illustrated.

3.1 Cellular Logic Computation

For a given configuration $\mathcal{A}_i$ or $\mathcal{B}_i$, we can use each state in the state set as a mask to represent a detecting expression in one of two canonical forms. Let $I \in \mathcal{G}(K(x))$ be a state, $I_i \in \{0,1\}$, $x_i^{I_i} = (x_i \neq I_i) = (\neg x_i \cap I_i) \cup (x_i \cap \neg I_i)$ and $x_i^{\neg I_i} = (x_i \equiv I_i) = (x_i \cap I_i) \cup (\neg x_i \cap \neg I_i)$. The detecting expression for x point needs to contain all variables in $K(x)$. An expression can be denoted by either $CL(K(x), \mathcal{A}_j)$ or $CL(K(x), \mathcal{B}_j)$.

In convenience, let $x_6 = x$ and $x_i, I_i \in \{0,1\}, i \in \{0, \cdots, 6\}$ and let y_j be a detecting function of the j-th configuration for 1-block edges and $\tilde{y}_j$ be a detecting function of the j-th configuration for 0-block edges, $j \in \{0,1,2\}$. We have two expressions.

$$
\begin{aligned}
y_j &= CL(K(x), \mathcal{A}_j) && (10)\\
&= \cup_{I \in \mathcal{A}_j} (\cap_{i=0}^{6} x_i^{I_i});\\
\tilde{y}_j &= CL(K(x), \mathcal{B}_j) && (11)\\
&= \cap_{I \in \mathcal{B}_j} (\cup_{i=0}^{6} x_i^{\neg I_i}).
\end{aligned}
$$

It is evident that the first detecting expression determines a 1 block edge point and the second expressions determines a 0 block edge point on the image. There is one-one corresponding relationship between a configuration of block edge detection and a detecting expression in cellular logic computation. However it is well known that there is no simple method to simplify a canonical Boolean expression into its optimal form when the expression contains rotational invariant classes [Dougherty 1992, Serra 1982]. For most applications, it is most convenient to use two canonical expressions. Owing to intrinsic difficulties of simplification of cellular logic expressions, it is reasonable to assume that a running time measurement of a detecting function is proportional to the number of states contained.

3.2 Conjugate Functions for Block Edge Detections

The third level of the conjugate classification uses three invariants: (x, p, q) representing different classes of the state set, Two parameters p and q are not Boolean variables. It is necessary to use arithmetical operations representing the respected expression.

For any class of the third level of the conjugate classification, there are three parameters (x, p, q): conjugation, connection and branch, $x \in \{0,1\}, p \in \{0, 1, \cdots, 6\}$ and $q \in \{0, 1, 2, 3\}$. Three configurations correspond to $p = q$, $p \geq 1$ plus $q = 2, q = \{3, 4\}$ conditions.

Two parameters p and q can be evaluated by following expressions.

$$p = \sum_{i=0}^{5}(x_i \neq x); \tag{12}$$

$$q = \frac{1}{2}\sum_{i=0}^{5}(x_i \equiv x_{i+1 \pmod 6}). \tag{13}$$

In order to describe the selected nodes of 1 or 0 block edge points, we can use the following expressions to project each (x, p, q) index into a 0-1 value.

Let $\{\equiv, \neq, \leq, \geq\}$ be arithmetic logic operations. For any x and y,

$$x \equiv y = \begin{cases} 1, & \text{if } x = y; \\ 0, & \text{otherwise.} \end{cases}$$

$$x \neq y = \begin{cases} 1, & \text{if } x \neq y; \\ 0, & \text{otherwise.} \end{cases}$$

$$x \leq y = \begin{cases} 1, & \text{if } x \leq y; \\ 0, & \text{otherwise.} \end{cases}$$

$$x \geq y = \begin{cases} 1, & \text{if } x \geq y; \\ 0, & \text{otherwise.} \end{cases}$$

Using four operations plus three Boolean logic operations, we can express all three configurations of 0 or 1 block edges through six functions.

Using the same y_j (or $\tilde{y}_j$) function as output value for a 1 (or 0) block edge point of the j-th configuration and any configuration $\mathcal{A}_i$ (or $\mathcal{B}_i$), let $y_i = CT(K(x), \mathcal{A}_i)$ (or $\tilde{y}_i = CT(K(x), \mathcal{B}_i)$) denote the detection function for the given condition, We have six functions (**Type A**).

$$y_0 = CT(K(x), \mathcal{A}_0) \tag{14}$$

$$
\begin{aligned}
&= ((x \equiv 1) \cap (q \equiv 1) \cap (p \equiv 2)) \cup ((x \equiv 1) \cap (q \equiv 1) \cap (p \equiv 3)) \cup \\
&\quad ((x \equiv 1) \cap (q \equiv 1) \cap (p \equiv 4)) \cup ((x \equiv 1) \cap (q \equiv 1) \cap (p \equiv 5));
\end{aligned}
$$

$$
\begin{aligned}
y_1 &= CT(K(x), \mathcal{A}_1) && (15)\\
&= y_0 \cup ((x \equiv 1) \cap (q \equiv 2) \cap (p \equiv 4));\\
y_2 &= CT(K(x), \mathcal{A}_2) && (16)\\
&= y_1 \cup (x \equiv 1) \cap (q \equiv 2) \cap (p \equiv 3));\\
\tilde{y}_0 &= CT(K(x), \mathcal{B}_0) && (17)\\
&= ((x \neq 1) \cup (q \neq 1) \cup (p \neq 2)) \cap ((x \neq 1) \cup (q \neq 1) \cup (p \neq 3)) \cap\\
&\quad ((x \neq 1) \cup (q \neq 1) \cup (p \neq 4)) \cap ((x \neq 1) \cup (q \neq 1) \cup (p \neq 5));\\
\tilde{y}_1 &= CT(K(x), \mathcal{B}_1) && (18)\\
&= \tilde{y}_0 \cap ((x \neq 1) \cup (q \neq 2) \cup (p \neq 4));\\
\tilde{y}_2 &= CT(K(x), \mathcal{B}_1) && (19)\\
&= \tilde{y}_1 \cap ((x \neq 1) \cup (q \neq 2) \cup (p \neq 3)).
\end{aligned}
$$

The six functions can be simplified further (**Type B**). That is,

$$
\begin{aligned}
y_0 &= CT(K(x), \mathcal{A}_0) && (20)\\
&= (x \equiv 1) \cap (q \equiv 1) \cap (p \geq 2);\\
y_1 &= CT(K(x), \mathcal{A}_1) && (21)\\
&= y_0 \cup ((x \equiv 1) \cap (q \equiv 2) \cap (p \equiv 4));\\
y_2 &= CT(K(x), \mathcal{A}_2) && (22)\\
&= y_0 \cup ((x \equiv 1) \cap (q \equiv 2) \cap (p \geq 3));\\
\tilde{y}_0 &= CT(K(x), \mathcal{B}_0) && (23)\\
&= ((x \neq 1) \cup (q \neq 2) \cup (p < 2));\\
\tilde{y}_1 &= CT(K(x), \mathcal{B}_1) && (24)\\
&= \tilde{y}_0 \cap ((x \neq 1) \cup (q \neq 2) \cup (p \neq 4));
\end{aligned}
$$

$$\tilde{y}_2 = CT(K(x), \mathcal{B}_2) \tag{25}$$
$$= \tilde{y}_0 \cap ((x \neq 1) \cup (q \neq 2) \cup (p < 3)).$$

Compared the simplified expressions (**Type B**) and original expressions (**Type A**), it is evident that two functions $y_0, \tilde{y}_0$ can be simplified equivalent to involving one class and another two functions $y_2, \tilde{y}_2$ can also be reduced to contain two classes. Two intermediate functions $y_1, \tilde{y}_1$ can be expressed as two classes too. These situations inform us that not only could conjugate functions concentrate configurations using classes, but also their expressions could be further simplified depending on specific distributions among involving classes.

For three configurations, six functions from two cellular logic expressions are equivalent to six functions of the conjugate expressions.

Proposition 3.2.1 *The six detecting functions of the cellular logic expressions of three configurations for block edge detections correspond to the six detecting functions of the conjugate expressions.*

Proof: A pair of two corresponding functions contains the same state set. Multiple variables determine the same output values. They can be verified directly. □

Using the proposition, we have following corollaries.

Corollary 3.2.2 *x is a 1-block edge point of the i-th configuration, if $y_i = 1$; otherwise $y_i = 0$,* $0 \leq i \leq 2$.

Corollary 3.2.3 *x is a 0-block edge point of the i-th configuration, if $\tilde{y}_i = 0$; otherwise $\tilde{y}_i = 1$,* $0 \leq i \leq 2$.

Three functions correspond to 1 block edge points and another three functions determine 0 block edge points.

4 Complexity Analysis for Block Edge Detections

There are obvious differences between a cellular logic function and a conjugate function. A cellular logic function uses Boolean variables and logic operations, however a conjugate function uses hybrid

Boolean plus arithmetical variables and logic plus arithmetical logic operations. In modern computer, an instruction takes a unit time either a logic, arithmetical logic or simple arithmetical operation. In relation to this equivalence, we can just calculate how many binary operations are required in each function. Using these complexity measurements, it is sufficient to compare two corresponding functions theoretically. Let τ_B denote a unit time for a binary operation, τ_p, τ_q denote the number of binary operations evaluating p and q parameters, $T(CT(K(x), \mathcal{A}))$ denote the number of binary operations involved in CL and CT equations, $N = |\mathcal{A}_i| = |\mathcal{B}_i|$ be the number of states and $n = ||\mathcal{A}_i|| = ||\mathcal{B}_i||$ be the number of classes. We have following equations.

$$\begin{aligned} T(CL(K(x), \mathcal{A}_i)) &= T(CL(K(x), \mathcal{B}_i)) \\ &= 14 \times N \times \tau_B, 0 \leq i \leq 2; \end{aligned} \tag{26}$$

$$\begin{aligned} T_0(CT(K(x), \mathcal{A}_i)) &= T(CT(K(x), \mathcal{B}_i)), 0 \leq i \leq 2; \\ &= \tau_p + \tau_q = 14 \times \tau_B + 14 \times \tau_B \\ &= 28 \times \tau_B; \end{aligned} \tag{27}$$

$$\begin{aligned} T_1(CT(K(x), \mathcal{A}_i)) &= T(CT(K(x), \mathcal{B}_i)), 0 \leq i \leq 2; \\ &= 7 \times n \times \tau_B; \end{aligned} \tag{28}$$

$$\begin{aligned} T(CT(K(x), \mathcal{A}_i)) &= T_0(CT) + T_1(CT) \\ &= (28 + 7 \times n) \times \tau_B. \end{aligned} \tag{29}$$

Using $T(CL)$ and $T(CT)$ measurements, we can investigate a speed-up ratio between two equations. Let $Sp_i^{CL:CT} = T(CL)/T(CT)$ be a theoretical speed-up ratio of CL and CT for the i configuration. Three configurations correspond three speed-up ratios: $N_0 = 24, n_0 = 4$; $N_1 = 33, n_1 = 6$ and $N_2 = 45, n_2 = 8$

$$\begin{aligned} Sp_i^{CL:CT} &= 14 \times N_i/(28 + 7 \times n_i) \\ &= 2 \times N_i/(4 + n_i). \end{aligned} \tag{30}$$

$$Sp_0^{CL:CT} = 2 \times 24/(4+4) = 6; \tag{31}$$

$$Sp_1^{CL:CT} = 2 \times 33/(4+6) = 6.6; \tag{32}$$

$$Sp_2^{CL:CT} = 2 \times 45/(4+8) = 7.5. \quad (33)$$

From the equation of a speed-up ratio for two schemes, it is evident that the conjugate function could have a speed-up ratio 6-7.5 faster than the corresponding cellular logic function. To use further simplified forms of the equations, a higher speed-up ratio can be achieved. We have $N_0 = 24, n_0 = 1$; $N_1 = 33, n_1 = 2$ and $N_2 = 45, n_2 = 2$.

$$Sp_0^{CL:CT} = 2 \times 24/(4+1) = 9.6; \quad (34)$$

$$Sp_1^{CL:CT} = 2 \times 33/(4+2) = 11; \quad (35)$$

$$Sp_2^{CL:CT} = 2 \times 45/(4+2) = 15. \quad (36)$$

In general, three configurations have a theoretical speed-up ratio 6-15.

5 Using the Conjugate Functions

In order to illustrate the advantage of the conjugate functions for block edge detections, two sets of sample pictures of binary images for three configurations of block edge detections are shown in Figure 6 and Figure 7 for 1-block edges and 0-block edges respectively in Appendix A. The pictures are generated from an implemented prototype of the *conjugate transformation* of the hexagonal grid [Zheng and Maeder 1993]. The conjugate transformation can support any combination of the selected classes from the 22 nodes of the third level of the conjugate classification. In Figures 6-7, pictures (b)-(c) illustrate three configurations for 1 (or 0) block edges respectively. Pictures (b) are simple block edges; both pictures (c) contain more block edge points and two pictures (d) provide the most details of block edge points. A specific application can correspond to one of three configurations. Because of the capability of the class representation to efficiently identify states, the implementation of the conjugate transformation on the hexagonal grid is very efficient. A speed-up ratio 6-15 for real measurements, compared with the same activity (0 or 1 block edge detection) performed by a standard implementation of cellular logic functions, can be observed. Both theoretical and real speed-up ratios are illustrated. The results shown in Table 1 provide numerical measurements of the speed-up ratio

Table 1: Time Measurements of Two Schemes

Function	n_i	N_i	CT	CL	$Sp_{CL:CT}$	$Sp^{CL:CT}$	Sample
Full Edges	1	1	86	38	0.44	0.4	Fig.6&7(e)
One Class	1	6	86	230	2.6	2.4	
$i = 0$	4	24	146	970	6.6	6	Fig.6&7(b) Type A
$i = 0$	1	24	86	970	11.2	9.6	Fig.6&7(b) Type B
$i = 1$	6	33	186	1367	7.3	6.6	Fig.6&7(c) Type A
$i = 1$	2	33	105	1367	13	11	Fig.6&7(c) Type B
$i = 2$	8	45	226	1920	8.4	7.5	Fig.6&7(d) Type A
$i = 2$	2	45	105	1920	18.2	15	Fig.6&7(d) Type B

Note: n_i is the equivalent number of classes for the i-th configuration, N_i is the number of involved states, CT is the average number of time units taken by a conjugate function, CL is the average number of time units taken by a cellular logic function, $Sp_{CL:CT}$ is equal to CL/CT for a speed-up ratio of real measurements, $Sp^{CL:CT}$ is a speed-up ratio for theoretical measurements and *Sample* indicates sample figures.

of running times of two compared programs on Model: CMN-B001, IRIX 4.0.5 System V, Silicon Graphics Iris 4D/25. The unit of the measurement time is 1/60 second.

6 CONCLUSION

From both representation and implementation, the proposed solution of three configurations of block edge detections based on conjugate functions is superior to cellular logic functions in the condition of representing composed classes in multiple structuring patterns. Using the proper class information, the 48, 66 and 90 states of the structuring patterns for block edge detections can be drastically reduced to simple expressions. This detection, therefore, provides a general structural description of relationships between adjacent spatial data points and block edge points as a fundamental paradigm for image analysis and processing operations of binary images on the hexagonal grid.

Acknowledgements: The author would like to express gratitude for Mrs. Patrizia Rossi for editing and proofreading this paper.

References

Dougherty E.R. (1992). *An Introduction to Morphological Image Processing*, SPIE Optical Engineering Press.

Golay M.J.E. (1969). "Hexagonal Parallel Pattern Transformations" *IEEE Trans. Comput.* Vol.18, pp733-740.

Kong T.Y. and Rosenfeld A. (1989). "Digital topology: Introduction and survey" Comput. Vision Graphics Image Processing. **48**, pp357-393.

Pitas I. and Venetsanopoulos A. (1989). "Morphological Shape Decomposition," *IEEE Trans. Pattern Anal. Machine Intell.*, Vol. 11, No. 7, July, 1989.

Preston Jr K. and Duff M.J.B. (1984). *Modern Cellular Automata: Theory and Application* Plenum Press, New York.

Rosenfeld A. (1979). "Connectivity in digital pictures", JACM, **17**, pp146-160.

Shapiro L., MacDonald R. and Sternberg S. (1987). "Ordered Structural Shape Matching with Primitive Extraction by Mathematical Morphology," *Pattern Recognition*, Vol. 20, No. 1, 1987.

Zheng Z.J. and Maeder A.J. (1992). "The Conjugate Classification of the Kernel Form of the Hexagonal Grid", *Modern Geometric Computing for Visualization* eds by T.L. Kunii and Y. Shinagawa, Springer-Verlag, pp73-89.

Zheng Z.J. and Maeder A.J. (1993). "The Elementary Equation of the Conjugate Transformation for Hexagonal Grid", *Modeling in Computer Graphics*, eds by B. Falcidieno and T.L. Kunii, Springer-Verlag, pp21-42.

Zheng Z.J. (1993a). "A Necessary Condition for Block Edge Detection of Binary Images on the Hexagonal Grid", *Communicating with Virtual Worlds*, eds by N. M. Thalmann and D. Thalmann, Springer-Verlag, pp553-566.

Zheng Z.J. (1993b). "An Efficient Scheme for Simple Network Detection for Binary Images on the hexagonal Grid," submitted to IEEE TENCON '94, Special Session On COMPUTER GRAPHICS & APPLICATIONS, and Technical Report No. 93/195, Department of Computer Science, Monash University, 22p.

Zheng Z.J. (1993c), "Three Configurations of Network Detections for Binary Images of the Hexagonal Grid," submitted to Computer Graphics International'94, and Technical Report No. 93/194, Department of Computer Science, Monash University, Dec. 1993, 24p.

Zheng Z.J. (Thesis 1994). "The Conjugate Transformation of the Regular Plane Lattices for Binary Images", Ph.D Thesis, Jan. 1994, Department of Computer Science, Monash University.

Appendix A

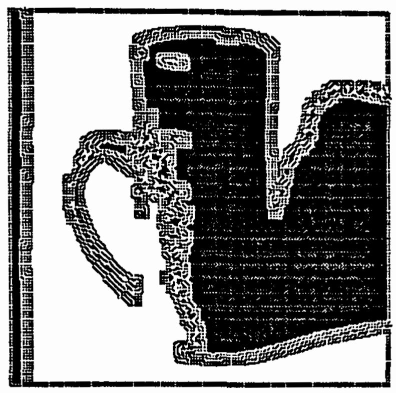

(a)

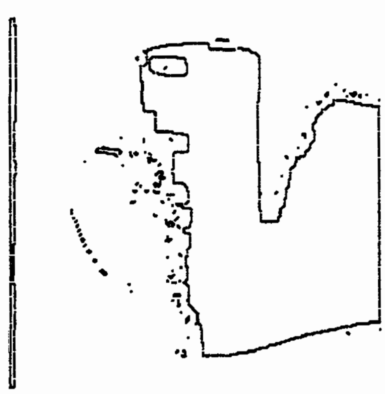

(b)

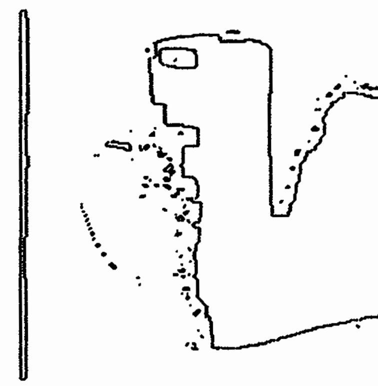

(c)

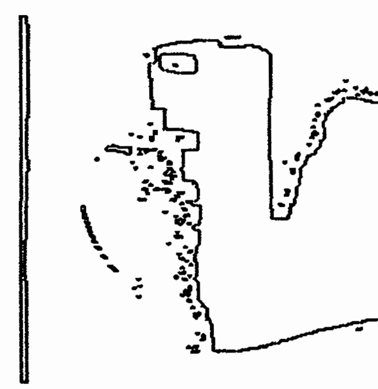

(d)

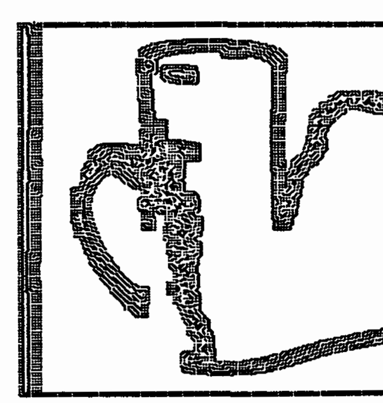

(e)

Figure 6: Sample Pictures of Black-ground (a)-(e). (a) original image (256 by 256), (b)-(e) sample images; (b) $\mathcal{A}_0$ Block Edge; (c) $\mathcal{A}_1$ Block Edge; (d) $\mathcal{A}_2$ Block Edge; (e) Full Edges for 1 Points.

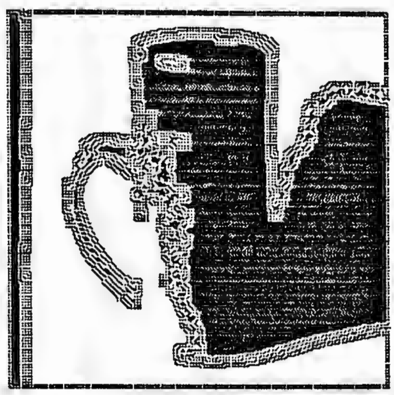

(a)

(b)

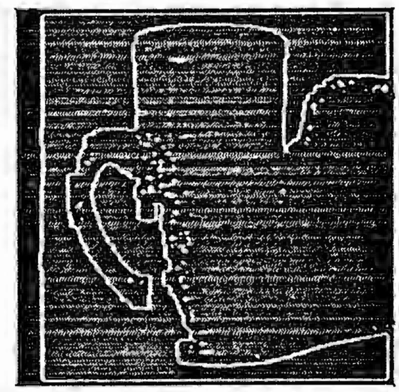

(c)

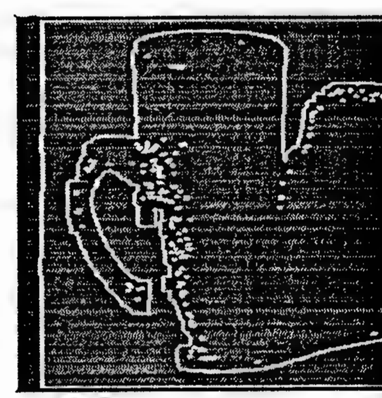

(d)

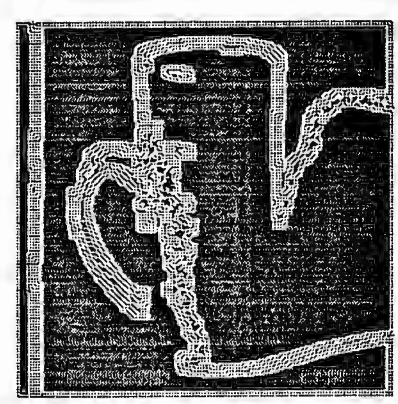

(e)

Figure 7: Sample Pictures of White-ground (a)-(e). (a) original image (256 by 256), (b)-(e) sample images; (b) $\mathcal{B}_0$ Block Edge; (c) $\mathcal{B}_1$ Block Edge; (d) $\mathcal{B}_2$ Block Edge; (e) Full Edges for 0 Points.